Available online at www.sciencedirect.com
SCIENCE DIRECT®
Journal of Catalysis 221 (2004) 110–118
JOURNAL OF CATALYSIS
www.elsevier.com/locate/jcat

Electrocatalytic synthesis of DMC over the Pd/VGCF membrane anode by gas–liquid–solid phase-boundary electrolysis

Ichiro Yamanaka,* Akiyasu Funakawa, and Kiyoshi Otsuka

Department of Applied Chemistry, Graduate School of Science and Engineering, Tokyo Institute of Technology, Ookayama, Meguro-ku, Tokyo 152-8552, Japan

Received 30 April 2003; revised 30 June 2003; accepted 11 July 2003

Abstract

Selective and efficient electrochemical carbonylation of MeOH to dimethyl carbonate (DMC) was investigated over a $PdCl_2$/VGCF (vapor-grown-carbon-fiber) membrane anode by three-phase-boundary electrolysis at 298 K. One of the advantages of this method is that it supplies higher P(CO) to the active site from the front side of the membrane anode and higher concentration of MeOH from the backside. The good performance of the DMC formation was obtained, 40 TON h^{-1}, 67% current efficiency, and 82% CO-selectivity under suitable conditions. Electrocatalysis of the $PdCl_2$/VGCF anode was studied by cyclic voltammetry and stoichiometric reactions between Pd^{2+}, MeOH, and CO. $PdCl_2$ on VGCF was reduced to the Pd^0 species with CO before the electrolysis and the Pd^0 species catalyzed direct electrochemical carbonylation of MeOH to DMC. On the other hand, oxidized Pd species on VGCF were assumed to catalyze the direct electrochemical carbonylation of MeOH to dimethyl oxalate (DMO).

Keywords: DMC; DMO; Carbonylation; Electrocatalysis; Oxidation; Membrane reactor; Pd; Methanol; CO

1. Introduction

Dimethyl carbonate (DMC) is one of the essential chemicals in the current chemical industry because DMC is expected to be a safe carbonylation reagent to substitute for the strong toxic reagents phosgene and dimethyl sulfate for the synthesis of carbamates, isocyanates, etc. [1]. A part of the DMC production, however, is manufactured by the phosgene method at present. Major production of DMC is manufactured by the EniChem method [2,3] and the Ube method [4] from MeOH and CO. The two industrial processes have the great advantage of no use of phosgene, compared with the phosgene method, but have disadvantages such as severe conditions and multistep operations. Therefore, it has been desired to develop a new reaction system for the one-step synthesis of DMC from MeOH and CO under mild conditions.

Several attractive methods for the electrochemical carbonylation of MeOH to DMC have been reported [5–8]. The productivities of DMC were low and the reaction conditions were severe. We have reported an electrochemical carbonylation method for DMC synthesis over a $PdCl_2$/graphite anode in the gas phase, as shown in Fig. 1a [9,10]. The assembly of the $PdCl_2$/graphite anode, the electrolyte membrane (H_3PO_4/H_2O in silica wool), and the Pt-black/graphite cathode was attached at the center of the gas electrolysis cell. A gas mixture of MeOH and CO was supplied over the anode at atmospheric pressure and 343 K. The electrochemical carbonylation of MeOH with CO to DMC was carried out by applying electrolysis voltages > 1.5 V. However, the performance for DMC formation was not excellent, with a selectivity of 11% based on CO, a current efficiency of 14%, and a turnover number (Pd) of 1 h^{-1}. Major products were CO_2, formed by the electrochemical oxidation of CO with H_2O, and dimethoxymethane (DMM) and methyl formate (MF) formed by electrochemical oxidation of MeOH [11]. Dimethyl oxalate (DMO) was not observed as one of the carbonylation products of MeOH. We concluded that the inferior performance in DMC formation was due to the low partial pressures (concentrations) of MeOH and CO on the anode and the high concentration of H_2O in the electrolyte membrane. In other word, increases in the concentrations of CO and MeOH and a decrease in the concentration of H_2O should strongly promote DMC formation [4,5].

* Corresponding author.
E-mail address: yamanaka@o.cc.titech.ac.jp (I. Yamanaka).

0021-9517/$ – see front matter
doi:10.1016/S0021-9517(03)00309-9

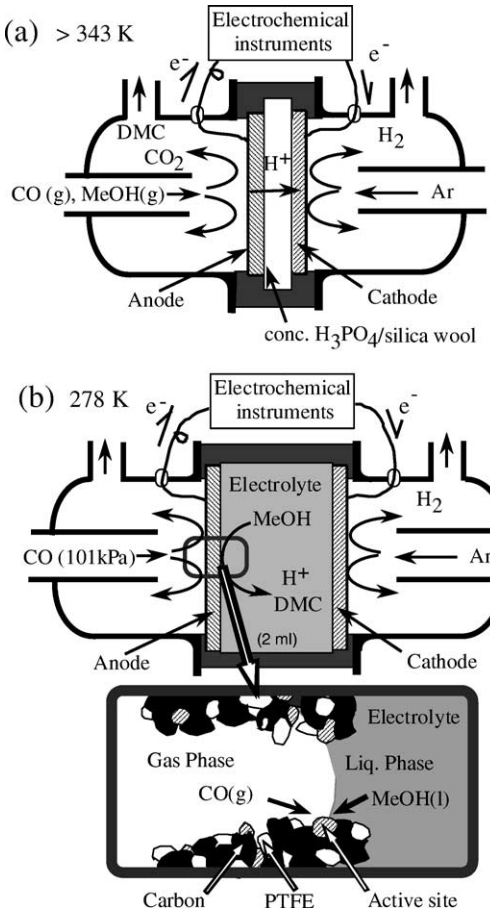

Fig. 1. Schematic diagrams of (a) gas-phase-electrolysis method and (b) three-phase-boundary electrolysis method for DMC formation.

We have proposed the new concept and the new cell structure for carbonylation to solve the above problems [12]. Our idea is utilization of the three-phase boundary of the gas phase (CO), the liquid phase (MeOH), and the solid phase (anode) for carbonylation, as shown in Fig. 1b. The solution of MeOH and electrolyte without H_2O fills the space between the porous membrane anode and cathode, and pure CO introduced to the opposite side of the anode. It was expected that the high partial pressure of CO (101 kPa), and the high concentration of MeOH (24.8 $\mathrm{mol\,l^{-1}}$) would be simultaneously supplied to the active site at the three-phase boundary in the anode and the selective synthesis of dimethyl carbonate (DMC) would be performed.

2. Experimental

2.1. Structure of the three-phase-boundary electrolysis cell

Figs. 2a and 2b show diagrams of the structure of the three-phase-boundary electrolysis cell for the DMC synthesis. The electrolysis cell was assembled from the porous membrane anode and cathode, the glass cells, the current collectors, the two PTFE gaskets A, the two PTFE gaskets B, the PTFE spacer, and the flange joints (Fig. 2b).

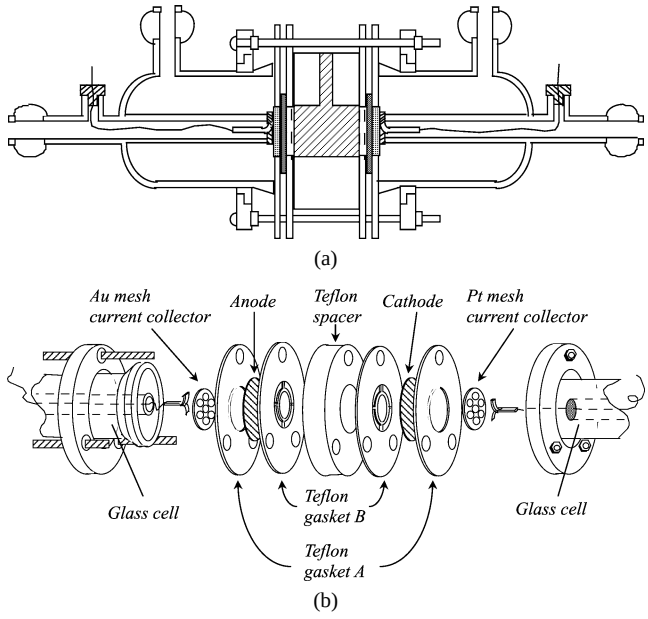

Fig. 2. Cell structure of three-phase-boundary electrolysis for DMC synthesis.

The porous membrane anode (0.2 mm thick) was prepared from electrocatalyst (50 mg) and PTFE powder (16 mg, Daikin Co.) by the hot-press method [13]. The electrocatalyst was prepared by the conventional impregnation method from $PdCl_2$/2HCl solution (1 $\mathrm{mmol\,l^{-1}}$) and vapor-growing carbon fiber (VGCF, 30 $\mathrm{g\,l^{-1}}$, Showa Denko Co.). The VGCF (specific surface area 13 $\mathrm{m^2\,g^{-1}}$) has high electron conductivity (0.015 $\Omega\,\mathrm{cm^{-1}}$) and good chemical stability (highly crystallized graphite structure) [14]. Therefore, the VGCF is expected the additives for the gas-diffusion electrodes for the fuel cell. The loading of Pd on the $PdCl_2$/VGCF catalyst was 3.5 g Pd/g VGCF. The porous membrane cathode (0.2 mm thick) was prepared by the same procedure from VGCF (50 mg), PTFE (5 mg), and Pt-black (20 mg, Wako Chemical Co.).

The porous membrane anode was sandwiched between the PTFE gaskets A and B, and the porous membrane cathode was also. The geometric areas of both electrodes were 1.5 $\mathrm{cm^2}$. The anode and cathode units were attached on both sides of the PTFE spacer. This electrolysis cell unit and the current collectors were sandwiched with the glass cells by flange joints with bolts and nuts (Fig. 2b).

2.2. Electrolysis procedures

The solution of MeOH and electrolyte (LiCl, $NaClO_4$, R_4NClO_4, etc.) fills the space (2 ml) between the porous membrane anode and cathode (Fig. 2a). A capillary salt bridge was inserted into the electrolyte. The capillary salt bridge was connected to the reference electrode (Ag|AgCl, 0.196 V vs NHE). A gas mixture of CO (0–101 kPa) and

He was passed through the anode and pure He was passed through the cathode. The total flow rates in the anode and cathode compartments were 15 ml min^{-1}, controlled by the mass-flow controllers.

The electrochemical carbonylation was started by applying an anode potential with a potentiostat-galvanostat (Hokuto HA-301) and a function generator (Hokuto HB-104) at 298 K. The current and the charge-passed were monitored by the zero-shunt ammeter (Hokuto HM-104A) and the coulomb meter (Hokuto HF-201).

Cyclic voltammetric studies for the anode were carried out using the same electrochemical instruments. The scan rate was 50 mV s^{-1}.

All reagents used in this work were special grade from Wako Chem. Co. and Aldrich Co. without further pulification.

2.3. Products analysis

Quantitative analysis of products in the liquid phase was carried out by a capillary gas chromatograph (Shimazu GC-14A with FID detector and PEG-20M capillary column) with a microsyringe every 30 min. Quantitative analysis of products in an gas phase was carried out by an on-line gas chromatograph (Shimazu GC-8A with TCD detector, Porapack-Q and AC columns) every 15 min.

The products in this work were DMC (dimethyl carbonate), DMO (dimethyl oxalate), DMM (dimethoxymethane), and MF (methyl formate) in the liquid phase and CO_2 in the gas phase. The reaction equations for the each product were estimated from the stoichiometric equations as

$$2CH_3OH + CO \rightarrow (CH_3O)_2CO + 2H^+ + 2e^-, \quad (1)$$

$$2CH_3OH + 2CO \rightarrow CH_3OC(O)C(O)OCH_3 + 2H^+ + 2e^-, \quad (2)$$

$$3CH_3OH \rightarrow (CH_3O)_2CH_2 + 2H^+ + 2e^- + H_2O, \quad (3)$$

$$2CH_3OH \rightarrow HC(O)OCH_3 + 4H^+ + 4e^-, \quad (4)$$

$$CO + H_2O \rightarrow CO_2 + 2H^+ + 2e^-. \quad (5)$$

The product selectivities were calculated on the basis of CO or MeOH. For example, the selectivities to DMC based on CO (CO-sel) and MeOH (MeOH-sel) were defined, respectively, as

$$\text{CO-sel} = \frac{\text{DMC (mol)} \times 100}{\text{DMC} + 2\text{DMO} + \text{CO}_2\ \text{(mol)}}\ (\%) \quad (6)$$

$$\text{MeOH-sel} = \frac{2\text{DMC (mol)} \times 100}{2\text{DMC} + 2\text{DMO} + 3\text{DMM} + 2\text{MF (mol)}}\ (\%). \quad (7)$$

The current efficiencies (CE) for products, DMC, DMO DMM, MF, and CO_2 were estimated from Eqs. (1)–(5). For example, the CE for DMC and DMO were defined, respectively as

$$\text{CE(DMC)} = \frac{2 \times \text{DMC formation rate (mol min}^{-1}) \times 96485\ (\text{C mol}^{-1})}{\text{coulomb (C min}^{-1})} \times 100\ (\%) \quad (8)$$

$$\text{CE(DMO)} = \frac{2 \times \text{DMO formation rate (mol min}^{-1}) \times 96485\ (\text{C mol}^{-1})}{\text{coulomb (C min}^{-1})} \times 100\ (\%). \quad (9)$$

2.4. Stoichiometric carbonylation of MeOH

The stoichiometric reaction between $PdCl_2$ (30 μmol) and MeOH (30 ml), and/or CO (101 kPa) in the presence of $NaClO_4$ (0.1 mol l^{-1}) was carried out in a conventional round bottom flask. The reaction mixture was stirred with a magnetic stir for 1 h at 298 K. The products were analyzed by the GC-techniques mentioned above.

3. Results and discussion

3.1. Screening of electrocatalyst

In our previous gas cell system, the screening test of various electrocatalysts (Pd-, Rh-, Ru-, Pt-, Ir-, Cu-, Ni-compounds) for DMC synthesis have been done at 343 K, and Pd and Cu elements were active for the electrochemical carbonylation of MeOH to DMC [9,10]. We examined the electrocatalysis of these elements for DMC synthesis by a new three-phase-boundary electrolysis cell at 298 K. The $PdCl_2$/VGCF anode was confirmed by the electrocatalysis for the DMC formation but the $CuCl_2$/VGCF anode was not in this work. We cannot answer the exact reason that the $CuCl_2$/VGCF anode was not active for carbonylation by the three-phase-boundary electrolysis, but the effect of the reaction temperature may be important for the electrocatalysis of the $CuCl_2$/VGCF anode. The electrocatalytic activities of some Pd species ($Pd(acac)_2$, $Pd(NO_3)_2$, $Pd(AcO)_2$, and Pd^0) supported on VGCF were examined but the formation rate, the CE, and the selectivity for the DMC formation were not so different. These results suggested that the real active Pd species are the same under the carbonylation conditions. We focused our interest on the electrocatalysis of the $PdCl_2$/VGCF anode for DMC synthesis by three-phase-boundary electrolysis.

3.2. Effects of electrolytes on the DMC synthesis

Fig. 3 shows the rough screening test of various electrolytes (0.05 mol l^{-1}) dissolved in MeOH on the carbonylation over the $PdCl_2$/VGCF anode (0.35 g Pd/g VGCF) applying a constant electrolysis voltage of 3.5 V at 298 K. The products dimethyl carbonate (DMC), dimethyl oxalate (DMO), dimethoxymethane (DMM), methyl formate (MF),

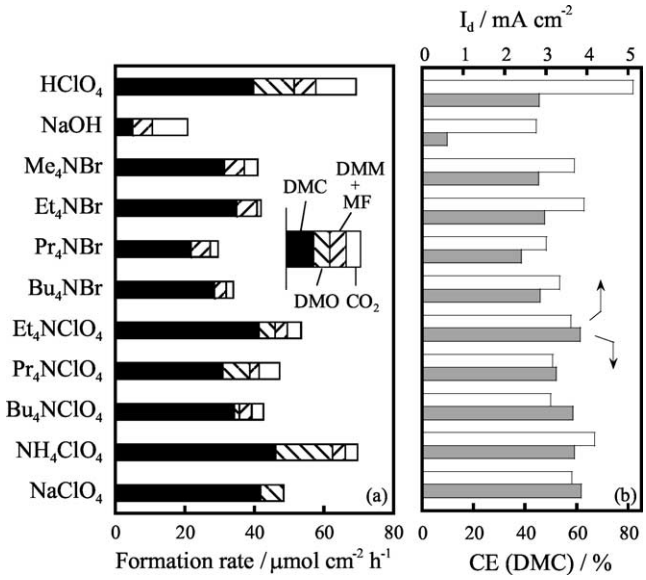

Fig. 3. Effects of various electrolytes on the electrochemical carbonylation of methanol over the $PdCl_2$/VGCF anode. $T = 298$ K; electrolysis voltage = 3.5 V; anode, $PdCl_2$ (0.35 Pd wt%)/VGCF; CO, 101 kPa; cathode, Pt/graphite; He, 101 kPa.

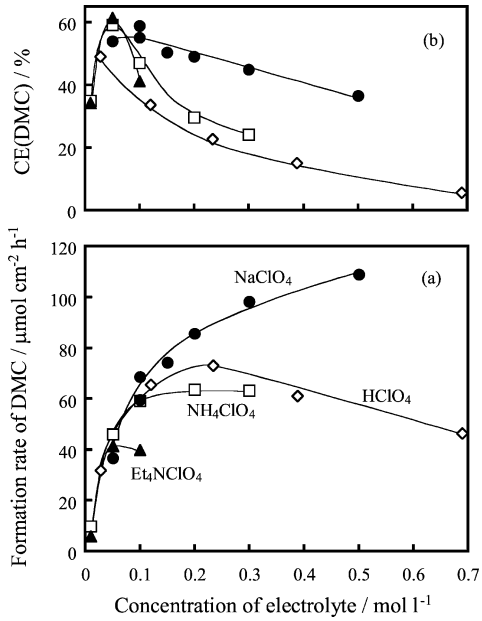

Fig. 4. Effects of the concentration of various electrolytes on (a) the DMC formation and (b) the current efficiency. Electrolysis voltage = 3.5 V; $T = 298$ K; anode, $PdCl_2$ (0.35 Pd wt%)/VGCF; CO, 101 kPa; cathode, Pt/graphite; He, 101 kPa. (●) $NaClO_4$, (□) NH_4ClO_4, (▲) Et_4NClO_4, (◇) $HClO_4$.

and CO_2 were determined by gas chromatography and the GC-mass spectroscopy. Other expected products, dimethyl ether and formic acid, were not detected in either the liquid phase or the gas phase.

Acid ($HClO_4$), base (NaOH), and neutral (ammonium bromide, ammonium perchlorate) electrolytes were used for the carbonylation. Good formation rates of DMC were observed for $HClO_4$ and neutral electrolytes but NaOH was not suitable. In the case of neutral electrolytes, high current efficiencies (CE) and low formation rates of (DMM + MF) and CO_2 were observed. Among the neutral electrolytes, Et_4NClO_4, NH_4ClO_4, and $NaClO_4$ were candidates for suitable electrolytes for selective DMC synthesis. No significant advantage for DMC synthesis among the three neutral electrolytes and $HClO_4$ was observed under the same concentration of electrolytes (0.05 mol l^{-1}). Therefore, influences of the concentration of electrolyte on the DMC synthesis were studied.

Fig. 4 shows the effects of the concentrations of Et_4NClO_4, NH_4ClO_4, $NaClO_4$, and $HClO_4$ electrolytes on the formation rate of DMC (a) and the CE (b). The upper limits of solubility of each neutral electrolyte in MeOH were different, 0.1 mol l^{-1} for Et_4NClO_4, 0.32 for NH_4ClO_4, and 0.54 for $NaClO_4$. As described in Fig. 3, differences among the four electrolytes were not clear for the DMC synthesis at the same electrolyte concentration of 0.05 mol l^{-1}. As you can see clearly in Fig. 4, the advantage of the $NaClO_4$ electrolyte became clear at higher concentrations. Higher formation rates of DMC and higher CE(DMC) were obtained with the $NaClO_4$ electrolyte than with the Et_4NClO_4, NH_4ClO_4, and $HClO_4$ electrolytes. At higher concentrations of the $HClO_4$ electrolyte, the formation rates of (DMM + MF) especially increased. When a small amount of H_2O was added to the $HClO_4$ electrolyte, the current density was increased but the formation rates of (DMM + MF) and CO_2 considerably increased. The unfavorable effect of the higher concentration of $HClO_4$ should be due to the increase in the concentration of H_2O contained $HClO_4$ reagent.

As described above, $NaClO_4$ was suitable for DMC synthesis. Therefore, details of the effect of the concentration of $NaClO_4$ on the carbonylation were studied, applying a constant electrolysis voltage of 3.5 V in Fig. 5. The current density increased with increasing the concentration of $NaClO_4$ because the ohmic resistance of the electrolyte decreased. Therefore, the formation rates of DMC increased with increasing in concentration of $NaClO_4$, corresponding to the current density. The higher formation rate of DMC was obtained at 0.5 mol l^{-1}, and the TON based on Pd for the DMC formation reached over 100 h^{-1}, as well as that of the Ube method [4].

The formation rate of DMO, a carbonylation product of MeOH, also increased with a similar tendency to DMC formation. The formation rates of (DMM + MF) and CO_2 increased at higher concentrations of $NaClO_4$. Therefore, the CO-sel and the MeOH-sel to DMC decreased at higher concentration of $NaClO_4$, though the formation rate of DMC increased (Fig. 5c). The suitable concentration of $NaClO_4$ was 0.1 mol l^{-1} because the high CE(DMC) of 59% and the high CO-sel of 66% to DMC were obtained.

3.3. Effects of $PdCl_2$ loading

Fig. 6 shows the effects of the $PdCl_2$ loading over the VGCF anode on the carbonylation using an $NaClO_4$ elec-

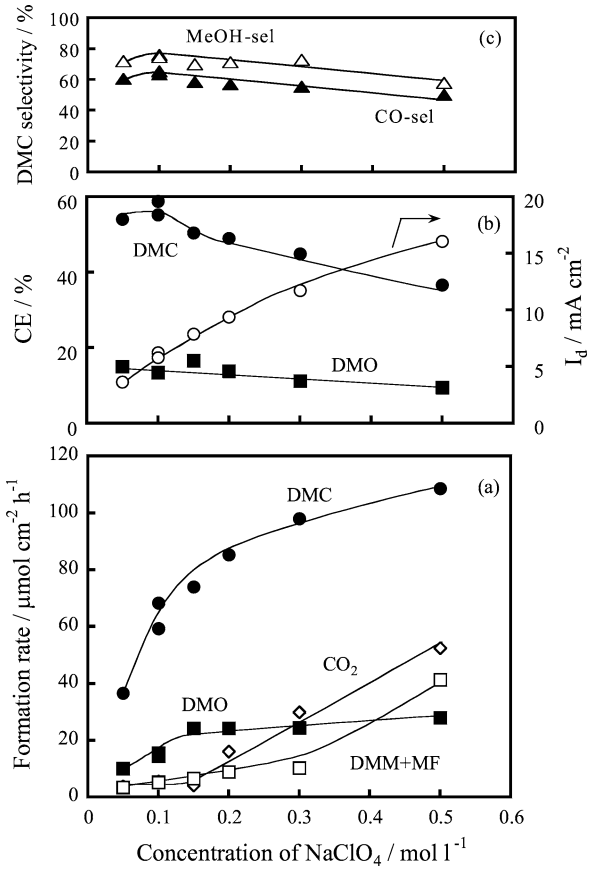

Fig. 5. Effects of concentration of $NaClO_4$ on (a) the DMC formation rate, (b) the current efficiency, and (c) the DMC selectivity. Electrolysis voltage = 3.5 V; $T = 298$ K; anode, $PdCl_2$ (0.35 Pd wt%)/VGCF; CO, 101 kPa; cathode, Pt/graphite; He, 101 kPa. (●) DMC, (■) DMO, (□) DMM + MF, (◇) CO_2, (▲) DMC selectivity (CO), (△) DMC selectivity (MeOH).

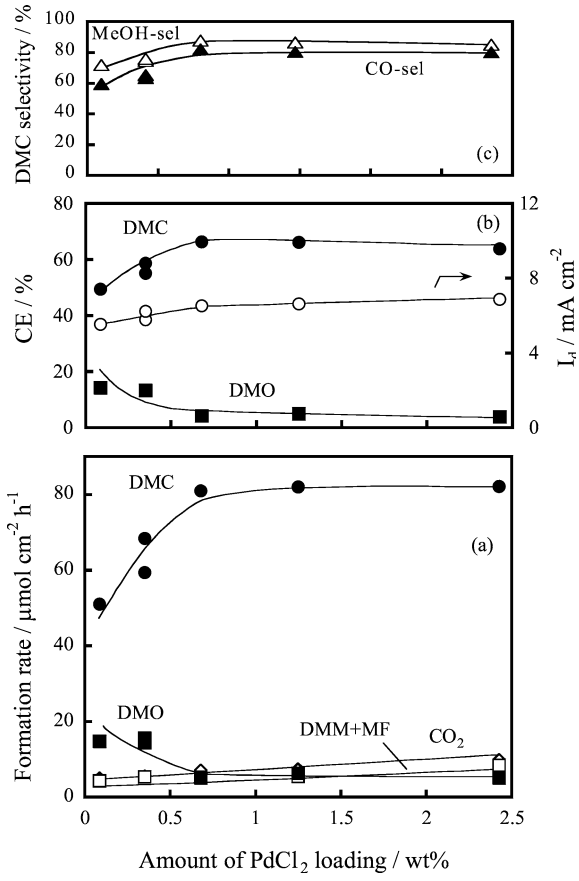

Fig. 6. Effects of the $PdCl_2$ loading over VGCF on (a) the DMC formation rate, (b) the current efficiency, and (c) the DMC selectivity. Electrolysis voltage = 3.5 V; $T = 298$ K; anode, $PdCl_2$/VGCF; CO, 101 kPa; cathode, Pt/graphite; He, 101 kPa; electrolyte, $NaClO_4$ (0.1 mol l^{-1})/CH_3OH. (●) DMC, (■) DMO, (□) DMM + MF, (◇) CO_2, (▲) DMC selectivity (CO), (△) DMC selectivity (MeOH).

trolyte of 0.1 mol l^{-1}, applying a constant electrolysis voltage of 3.5 V. The current density slightly increased with increasing $PdCl_2$ loading up to 0.7 Pd^0 wt%, but was almost constant above 0.7 Pd^0 wt%. The dependence of the $PdCl_2$ loading on the current density was weak. In contrast to the current density, the formation rate of DMC strongly depended on the $PdCl_2$ loading. The formation rate of DMC drastically increased with the $PdCl_2$ loading up to 0.7 Pd^0 wt% but showed the upper limit for the DMC formation rate. High CO-sel and MeOH-sel were obtained above 0.7 Pd^0 wt% (Fig. 6c). In contrast to the DMC formation, the formation rate of DMO increased with decreasing $PdCl_2$ loading. On the other hand, the formation rates of CO_2 and DMM + MF were almost constant without dependence of the $PdCl_2$ loading. We can obviously observe changing electrocatalysis of the $PdCl_2$/VGCF anode with changing CE in Fig. 6b. The changing of DMC and DMO selectivities are significant when the reaction mechanism of carbonylation over the $PdCl_2$/VGCF anode is considered. A very high TON (Pd) of 192 h^{-1} for the DMC formation was obtained at a $PdCl_2$ loading of 0.09 Pd^0 wt%, though the formation rate of DMO (56 TON h^{-1}) was fairly large.

The most effective $PdCl_2$ loading is around at 0.7 Pd^0 wt% because the highest formation rate, the highest CE of 67%, the highest CO-sel of 82%, and the highest MeOH-sel of 88% for the DMC formation were obtained. The $PdCl_2$ loading of 0.7 Pd^0 wt% was chosen as the suitable loading hereafter.

3.4. Optimum reaction conditions

Fig. 7 shows effects of the partial pressure of CO on the carbonylation, applying a constant electrolysis voltage of 3.5 V. The current densities slightly increased with P(CO) in Fig. 7b. Of course, the formation rates of DMC and DMO were zero at $P(CO) = 0$ kPa in Fig. 7a. The formation rate of DMC smoothly increased with increasing P(CO) and seemed to reach the upper limit at higher $P(CO) > 50$ kPa. The CO-sel and the MeOH-sel increased with P(CO) in Fig. 7c. Selective carbonylation of MeOH to DMC was performed at higher P(CO). This dependence of P(CO) on the DMC formation suggested that enough concentration of CO supplied to the active site in the porous membrane anode ($PdCl_2$/VGCF) at $P(CO) < 50$ kPa, which would be one

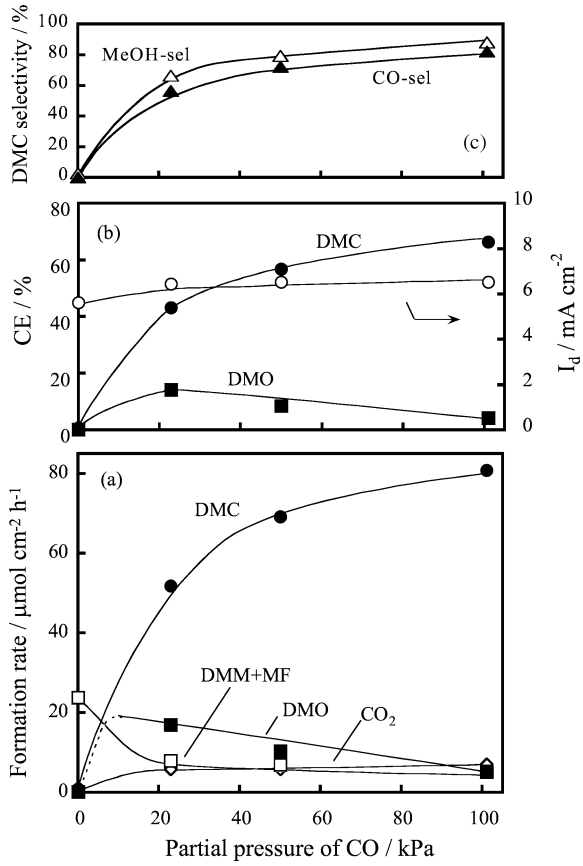

Fig. 7. Effects of partial pressure of CO on (a) the DMC formation rate, (b) the current efficiency, and (c) the DMC selectivity. Electrolysis voltage = 3.5 V; $T = 298$ K; anode, $PdCl_2$ (0.7 Pd wt%)/VGCF; cathode, Pt/graphite; He, 101 kPa; electrolyte, $NaClO_4$ (0.1 mol l^{-1})/CH_3OH. (●) DMC, (■) DMO, (□) DMM + MF, (◇) CO_2, (▲) DMC selectivity (CO), (△) DMC selectivity (MeOH).

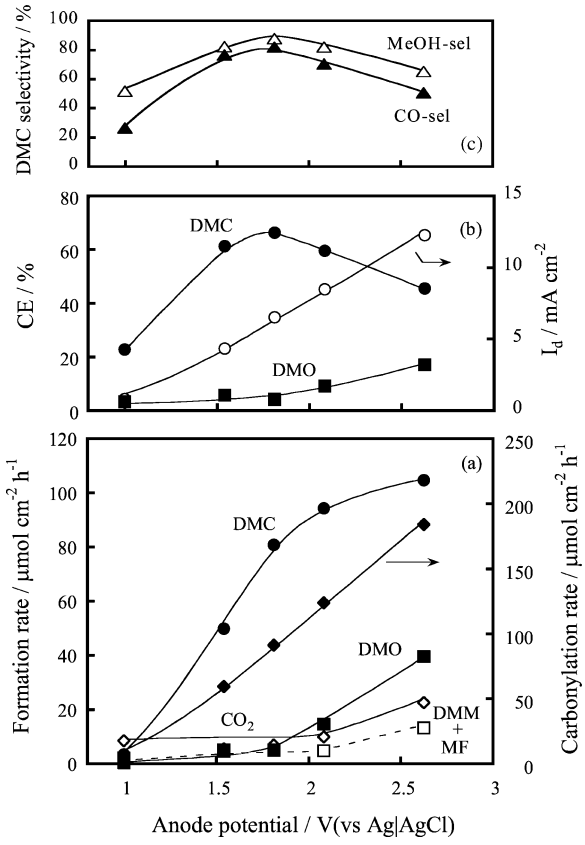

Fig. 8. Effects of anode potential on (a) the DMC formation rate, (b) the current efficiency, and (c) the DMC selectivity. $T = 298$ K; anode, $PdCl_2$ (0.7 Pd wt%)/VGCF; CO, 101 kPa; cathode, Pt/graphite; He, 101 kPa; electrolyte, $NaClO_4$ (0.1 mol l^{-1})/CH_3OH. (●) DMC, (■) DMO, (□) DMM + MF, (◇) CO_2, (▲) DMC selectivity (CO), (△) DMC selectivity (MeOH).

of the advantages of the three-phase boundary electrolysis method.

On the other hand, the formation rate of DMO decreased with increasing $P(CO) > 20$ kPa. This dependence was opposite to that of DMC. The dependence of $P(CO)$ on the formation rate of DMO was strange because two molecule of CO were necessary for the formation of DMO [Eq. (2)] but one for the DMC formation [Eq. (1)]. Therefore, stronger enhancement of $P(CO)$ on the formation rate of DMO was expected. However, the dependence of $P(CO)$ on the formation rate of DMO was negative. In addition, the formation rate of DMO might change discontinuously between $P(CO)$ of 20 and 0 kPa. On the other hand, the formation rate of (DMM + MF) was constant without dependence on $P(CO)$. The maximum formation rate of (DMM + MF) was obtained at $P(CO) = 0$ kPa with 33% CE. This fact suggested that the partial oxidation of MeOH was inhibited by the presence of CO. These experimental results suggested that the catalysis of the $PdCl_2$/VGCF anode and the activation mode of MeOH drastically changed with and without the presence of CO.

3.5. Electrocatalysis of the $PdCl_2$/VGCF anode

To obtained information for the electrocatalysis of the $PdCl_2$/VGCF for the carbonylation, the effects of anode potentials were studied, as shown in Fig. 8. A capillary salt bridge was connected to the cell to control the anode potential. The carbonylation of MeOH over the $PdCl_2$/VGCF anode was carried out under potentiostatic conditions (vs Ag|AgCl). The anode potential when the standard electrolysis voltage of 3.5 V was applied was +1.80 V (Ag|AgCl) using an $NaClO_4$ electrolyte (0.1 mol l^{-1}).

The current densities increased exponentially with increasing anode potentials above +1.0 V. The formation rate of DMC increased with a sigmoid curve for the anode potentials and reached an upper limit at around +2.6 V. In contrast to the DMC formation, the formation rate of DMO accelerated above +1.8 V. The carbonylation rate, the reaction rate of CO insertion to MeOH, which was estimated from the sum of the DMC formation rate and twice the DMO formation rate, increased exponentially with increasing in the anode potential. The CE(DMC) showed the maximum at +1.8 V and the CE(DMO) increased above +1.8 V. In addition, the formation rates of CO_2 and (DMM + MF) also

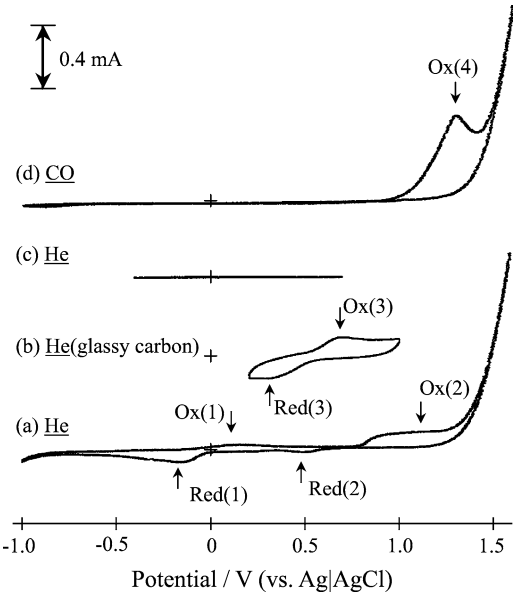

Fig. 9. Cyclic voltammograms over the Pd wire electrode (a, c, d) and glassy carbon electrode (b). Scan rate, 50 $mV\,s^{-1}$; electrolyte, $NaClO_4$ (0.1 $mol\,l^{-1}$)/CH_3OH (a) in He, (b) addition of $PdCl_2$, (c) in He ($-0.5 \leftrightarrow +0.7$ V), (d) in CO.

increased above +1.8 V, which corresponded to changing the MeOH-sel and the CO-sel as shown in Fig. 8c. These observations strongly suggest a change of the electrocatalysis of the $PdCl_2$/VGCF anode above +1.8 V.

To obtain more information for the electrochemical properties of the anode, cyclic voltammogram measurements (CV) of the $PdCl_2$/VGCF electrode were attempted, but significant CV spectra could not be obtained. Therefore, CV spectra of Pd-wire ($0.4\phi \times 10$ mm) were measured under very similar conditions for the carbonylations ($NaClO_4$ (0.1 $mol\,l^{-1}$)/MeOH), as shown in Fig. 9. The CV(a) spectra show redox properties of the Pd-wire swept with a wide window from −1.0 to +1.5 V in He. A few oxidation peaks, the Ox(1) at +0.1 V and the Ox(2) at +0.85 V, and reduction peaks, the Red(1) at −0.2 V and the Red(2) at +0.5 V, were observed. A large oxidation current was observed above +1.3 V. This large oxidation current should be electrochemical oxidation of MeOH to DMM and MF. The Ox(1) and the Red(1) peaks seem to be the redox couple. The broad oxidation peak of the Ox(2) and the small reduction peak of the Red(2) may be the redox couple but most of the oxidation current in the broad Ox(2) peak was for the irreversible reaction. In the CV(b), we observed the redox couple of Pd^{2+}/Pd^0, Ox(3)/Red(3), in the $PdCl_2 \cdot 2HCl$/MeOH solution over the glassy carbon electrode. The redox potential of Pd^{2+}/Pd^0 estimated roughly from the CV(b) was not so far from that of Ox(2)/Red(2) in the CV(a). The broad irreversible oxidation current in the Ox(2) should be for the oxidation of Pd-wire to Pd^{2+} species. Pd^0 may be electrochemically oxidized with MeOH and form $Pd^{2+}(MeO^-)_x$ species and H^+,

$$Pd^0 + x\,MeOH \rightarrow Pd^{2+}(MeO^-)_x + x\,H^+. \quad (10)$$

This Pd^{2+} species diffuse to the bulk solution. Therefore, the Ox(2) peak and the Red(2) peak become asymmetric. To obtain information for the redox couple of Ox(1)/Red(1), the sweep was reduced from −0.5 to +0.7 V, CV(c). No oxidation and reduction current was observed. This observation suggested that the Ox(1)/Red(1) couple was correlated to the oxidation current in the Ox(2). The Ox(1)/Red(1) couple may correspond to the reduction of H^+ produced at Eq. (10) to H(a) and the oxidation of H(a) to H^+; however, this might not be relevant to the carbonylation because the potential might be too low. In conclusion, the CV of Pd-wire was measured in CO, CV(d). A large oxidation peak at +1.2 V (Ox(4)) was observed. The large oxidation current above +1.4 V should be due to the oxidation of MeOH, as observed in the CV(a). No reduction peaks corresponding to the Red(2) in the CV(a) and the redox couple of Ox(1)/Red(1) at low potential (CV(a)) were observed. The Ox(4) peak should correspond to the oxidation of CO or the oxidative insertion of CO to MeOH. The absence of a reduction peak in the CV(d) corresponding to the Red(2) suggested that Pd-wire did not oxidize to Pd^{2+} species above +1.0 V in CO. The reduction state of Pd was stable in CO. In addition, the absence of a reduction peak in CV(d) corresponding to the Red(1) in the CV(a) should be due to the inhibition of the H^+ adsorption by the strong adsorption of CO over Pd^0. These results suggested that the electrochemical carbonylation was catalyzed by Pd^0 species.

However, the active $PdCl_2$/VGCF anode was prepared from the $PdCl_2$/2HCl solution and VGCF by the conventional impregnation method without reduction treatment. The oxidation state of Pd species over the VGCF should be Pd^{2+} after the preparation of the $PdCl_2$/VGCF electrode. Pd^0 or Pd^{2+}: which oxidation state is active for the DMC synthesis? On the basis of previous work [15], the Pd^{2+}/Pd^0 redox would catalyze the electrochemical carbonylation of MeOH. If Pd^{2+} was active species for the carbonylation in this reaction system, the stoichiometric carbonylation of MeOH with CO by Pd^{2+} (oxidant) was expected. In this case, the electrochemical potential is for the oxidation of Pd^0 to Pd^{2+}. If Pd^0 was active species for the carbonylation, the direct electrochemical carbonylation would proceed. Therefore, the stoichiometric reactions between MeOH, CO, H_2O, and Pd^{2+} is studied in Table 1.

Table 1 shows the stoichiometric reaction between Pd^{2+} and MeOH, and/or CO in the presence of $NaClO_4$ at 298 K. Entry 1 shows the stoichiometric reaction between $PdCl_2$, MeOH, and CO. This reaction conditions were very near to the electrochemical carbonylation conditions, except for applying the electrochemical potential. As you can see clearly, no formation of DMC was observed but CO_2 was formed with this high yield of 88% based on Pd^{2+}. In entry 2, the oxidation of MeOH by Pd^{2+} was carried out but no oxidation of MeOH, no formation of DMM and MF, was observed. On the other hand, the stoichiometric oxidation of CO to CO_2 with H_2O by Pd^{2+} (99% yield) proceeded in entry 3.

Table 1
Stoichiometric reaction between Pd^{2+}, MeOH, and CO

Entry		Amount of products (μmol)				
		DMC	DMO	DMM	MF	CO_2
1	$PdCl_2 + CO + CH_3OH$	0	0	trace	0	26.4
2	$PdCl_2 + He + CH_3OH$	0	0	0	0	0
3	$PdCl_2 + CO + H_2O$	0	0	0	0	29.7
4	$PdCl_2/AC + CO + CH_3OH$	0	0	trace	2.2	0

$T = 298$ K; reaction time = 1 h; CO, 101 kPa; H_2PdCl_4; 30 μmol, MeOH, 30 ml.

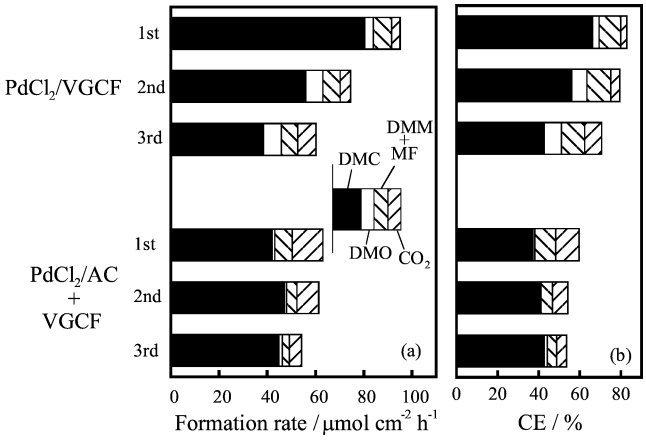

Fig. 10. Stabilities of the $PdCl_2$/VGCF and the [$PdCl_2$/AC + VGCF] anodes for the carbonylation of MeOH. Electrolysis voltage = 3.5 V; $T = 298$ K; anode, $PdCl_2$ (0.7 Pd wt%)/VGCF; CO, 101 kPa; cathode, Pt/graphite; He, 101 kPa; electrolyte, $NaClO_4$ (0.1 mol l^{-1})/CH_3OH.

These experimental results suggest that the carbonylation of MeOH with CO to DMC by Pd^{2+} did not proceed but the oxidation of CO to CO_2 proceeded through

$$Pd^{2+} + CO + H_2O \rightarrow Pd^0 + CO_2 + 2H^+. \quad (11)$$

Therefore, Pd^{2+} species on the $PdCl_2$/VGCF anode should be reduced to Pd^0 with CO before the electrolysis [Eq. (11)]. This model correspond to the observation of the CV(d) in Fig. 9, no reduction peak of Pd^{2+} in CO. Pd^0 species on VGCF would be active species for the electrochemical carbonylation of MeOH to DMC. The exact expression of the $PdCl_2$/VGCF anode is the Pd^0/VGCF anode.

3.6. Development of stable anode

Fig. 10 shows the stabilities of the $PdCl_2$/VGCF (Pd^0/VGCF) anode for carbonylation. The same anode was used repeatedly three times for the carbonylation. The electrolyte solutions and the cathode were changed to new ones at each experiment. The yields of DMC decreased with run numbers of the experiments. The current efficiencies also decreased with experimental numbers. A small amount of black powder deposition was observed on the bottom of the cell after the electrolysis. These facts suggested that the Pd^0 species on VGCF should be oxidized and desorbed into the electrolyte bulk phase during the electrolysis.

To develop the stable anode, $PdCl_2$ was supported on the active carbon (AC, Wako Co.) by the conventional impregnation method because the AC has a very high specific surface area (900 $m^2\,g^{-1}$) and good adsorption ability. The new anode was prepared from $PdCl_2$/AC powder (5 wt%, 20 mg), VGCF (50 mg), and PTFE (16 mg) by the hot-press method. The formation rate of DMC over the ($PdCl_2$/AC + VGCF) anode in the first run was lower than that of the $PdCl_2$/VGCF anode. However, the formation rates of DMC in the second and third runs were as high as that in the first run for the ($PdCl_2$/AC + VGCF) anode. The CE(DMC) were also constant though that of 40% was slightly low. In addition, no black deposition was observed on the bottom of the cell. These facts proposed that the ($PdCl_2$/AC + VGCF) anode was stable for the carbonylation of MeOH to DMC.

To obtain information on the active form of Pd species on the $PdCl_2$/AC + VGCF anode, XRD spectra were measured. XRD patterns at $2\theta = 40°$ and 46° were observed for the $PdCl_2$/AC electrocatalyst, which was assigned to Pd^0(111) and Pd^0(200) by the JCPDS data. This result suggested that $PdCl_2$ was reduced to Pd^0 during the preparation procedure of the electrocatalyst. For the stoichiometric reaction between $PdCl_2$/AC, CO, and MeOH at Entry 4 in Table 1, no formation of CO_2 was observed, which suggested the absence of Pd^{2+} on the $PdCl_2$/AC. On the other hand, no XRD patterns were assigned to Pd^0 on the $PdCl_2$/VGCF anode. These results suggested that the AC support stabilized the state of Pd^0 more than the VGCF support.

3.7. Reaction scheme

A model of the reaction scheme in this reaction system is shown in Fig. 11. The three-phase boundary of the gas phase (CO), the liquid phase (MeOH), and the solid phase (Pd/VGCF anode) was significant for the effective and selective carbonylation of MeOH. A high partial pressure of CO from the front side of the membrane anode and a high concentration of MeOH from the backside were simultaneously supplied to the active site in the anode (Figs. 1, 11(1)). $PdCl_2$ species on the anodes ($PdCl_2$/VGCF and $PdCl_2$/AC + VGCF) reduced to Pd^0 species with a high partial pressure of CO (Fig. 11(2)). The electrochemical carbonylation of MeOH with CO proceeded on Pd^0-supported VGCF and AC. This reaction is direct electrochemical carbonylation, not indirect electrochemical carbonylation through the Wacker-type redox reaction of Pd^{2+}/Pd^0, because stoi-

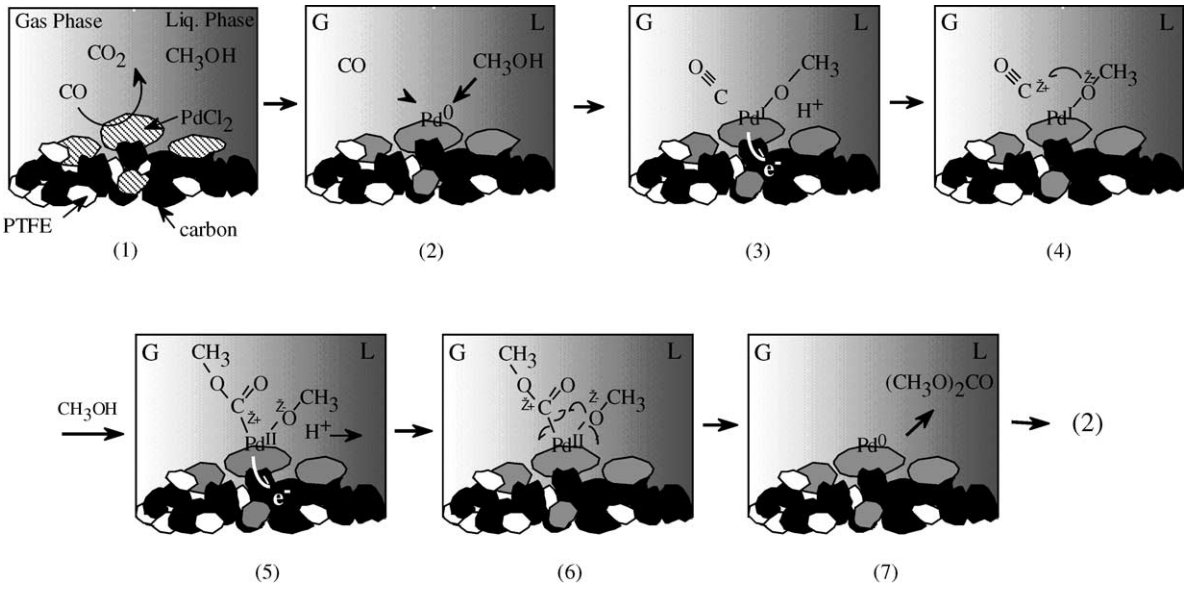

Fig. 11. A reaction scheme for the carbonylation of MeOH by three-phase-boundary electrolysis.

chiometric DMC formation between Pd^{2+}, MeOH, and CO did not proceed in this reaction conditions (Table 1). On the basis of previous reports [9,10] and the carbonylation chemistry [1–4], a model of the reaction mechanism for the carbonylation of MeOH could be speculated in Fig. 11(3–6), (3) formation of the methoxy group on Pd (Pd(I) (MeO^-) (CO)), (4) insertion of CO into the methoxy group on Pd, (5) and (6) insertion of the methoxy group into the methoxy carbonyl group on Pd, and (7) desorption of DMC from Pd.

On the other hand, the formation rate of DMO and the CE(DMO) increased at lower $PdCl_2$ loading in Fig. 6, at lower P(CO) in Fig. 7, and at higher anode potential in Fig. 8. These conditions may be favorable for the formation of oxidized Pd species (Pd^{2+}). In addition, no formation of DMO was observed through the stoichiometric reaction between MeOH, CO, and Pd^{2+} (Table 1). Therefore, oxidized Pd species (Pd^{2+}) on VGCF or AC would catalyze the direct electrochemical carbonylation of DMO.

In addition, the formation of DMM and MF should proceed through the direct electrochemical oxidation of MeOH [16,17]. The low selectivities to DMM, MF, and CO_2 were due to the low concentration of H_2O in the electrolyte/MeOH solutions. The equivalent formation of H_2 was confirmed at the cathode, corresponding to the carbonylation (Eqs. (1) and (4)) and the oxidation (Eqs. (2) and (3)).

4. Conclusions

As described so far, the advantage of the three-phase-boundary electrolysis method is supplying a higher partial pressure of CO from the front side of the Pd/VGCF membrane anode and a higher concentration of MeOH from the backside to the active site, simultaneously. The effective and selective carbonylation of MeOH to DMC under mild conditions was performed by the three-phase-boundary electrolysis with neutral electrolyte containing less water (maxima values: TON(Pd) of 192 h^{-1}, CO-sel of 82%, MeOH-sel of 88%). This performance for the DMC formation was drastically improved to compare with our previous results [9,10]. Pd^0 species on VGCF catalyzed the direct electrochemical carbonylation of MeOH to DMC and oxidized Pd species, maybe Pd^{2+}, was proposed to catalyze the direct electrochemical formation of DMO. These results proposed that the possibility of electrochemical control of the carbonylation selectivities to DMC and DMO. The principle of the three-phase-boundary electrolysis method could apply to other electrosynthesis [18].

References

[1] P. Tundo, M. Selva, Acc. Chem. Res. 35 (2002) 706.
[2] U. Romano, R. Tesel, M.M. Maurl, P. Rebora, Ind. Eng. Chem. Prod. Res. Dev. 19 (1980) 396.
[3] U. Romano, Chem. Ind. 75 (1993) 303.
[4] T. Matsuzaki, A. Nakamura, Catal. Surv. Jpn. 1 (1997) 77.
[5] D. Cipris, I.L. Mador, J. Electrochem. Soc. 125 (1978) 1954.
[6] R.A. Dombro Jr., G.A. Prentice, M.A. McHugh, J. Electrochem. Soc. 135 (1978) 2219.
[7] A. Galia, G. Filardo, S. Gambino, R. Mascolino, F. Rivetti, G. Silvestri, Electrochim. Acta 41 (1996) 2893.
[8] G. Filardo, A. Galia, F. Rivetti, O. Scialdone, G. Silvestri, Electrochim. Acta 42 (1997) 1961.
[9] K. Otsuka, T. Yagi, I. Yamanaka, Electrochim. Acta 39 (1994) 2109.
[10] K. Otsuka, T. Yagi, I. Yamanaka, Chem. Lett. (1994) 495.
[11] I. Yamanaka, K. Otsuka, Electrochim. Acta 34 (1989) 211.
[12] I. Yamanaka, A. Funakawa, K. Otsuka, Chem. Lett. (2002) 448.
[13] I. Yamanaka, A. Nishi, K. Otsuka, Catal. Today 66 (2001) 115.
[14] Available at: http://www.sdk.co.jp/index.htm.
[15] I.L. Mador, A.U. Blackham, US Patent 3114762, 1963.
[16] K. Otsuka, I. Yamanaka, Appl. Catal. 26 (1986) 401.
[17] K. Otsuka, I. Yamanaka, Electrochim. Acta 34 (1989) 211.
[18] I. Yamanaka, T. Hashimoto, K. Otsuka, Chem. Lett. (2002) 852.